Thermodynamic Characterization of Three Polymorphic Forms of Piracetam

RICARDO PICCIOCHI,[1] HERMÍNIO P. DIOGO,[1] MANUEL E. MINAS da PIEDADE[2]

[1]Centro de Química Estrutural, Complexo Interdisciplinar, Instituto Superior Técnico, 1049-001 Lisboa, Portugal

[2]Departamento de Química e Bioquímica, Faculdade de Ciências, Universidade de Lisboa, 1749-016 Lisboa, Portugal

Received 4 May 2010; revised 15 June 2010; accepted 16 June 2010

Published online 1 October 2010 in Wiley Online Library (wileyonlinelibrary.com). DOI 10.1002/jps.22294

ABSTRACT: Combustion calorimetry, solution calorimetry, and differential scanning calorimetry (DSC) were used to determine the standard ($p^\circ = 0.1$ MPa) molar enthalpies of formation of Forms I, II, and III piracetam at 298.15 K, namely, $\Delta_f H_m^\circ$ ($C_6H_{10}O_2N_2$, cr I) = -520.6 ± 1.6 kJ·mol^{-1}, $\Delta_f H_m^\circ$ ($C_6H_{10}O_2N_2$, cr II) = -523.8 ± 1.6 kJ·mol^{-1}, and $\Delta_f H_m^\circ$ ($C_6H_{10}O_2N_2$, cr III) = -524.1 ± 1.6 kJ·mol^{-1}. The enthalpy of formation of gaseous piracetam at 298.15 K was also derived as $\Delta_f H_m^\circ$ ($C_6H_{10}O_2N_2$, g) = -401.3 ± 2.1 kJ·mol^{-1}, by combining the standard molar enthalpy of formation of Form II piracetam with the corresponding enthalpy of sublimation, $\Delta_{sub} H_m^\circ$ ($C_6H_{10}O_2N_2$, cr II) = 122.5 ± 1.4 kJ·mol^{-1}, obtained by drop-sublimation Calvet microcalorimetry and the Knudsen effusion method. The $\Delta_f H_m^\circ$ ($C_6H_{10}O_2N_2$, g) value was used to assess the corresponding predictions by the B3LYP/cc-pVTZ (-335.3 kJ·mol^{-1}), G3MP2 (-388.7 kJ·mol^{-1}), and CBS-QB3 (-402.8 kJ·mol^{-1}) methods, based on the calculation of the atomization enthalpy of piracetam. Finally, the results of the solution and DSC experiments indicate that the stability hierarchy of Forms I, II, and III piracetam at 298.15 K, for which there was conflicting evidence in the literature, is III > II > I. © 2010 Wiley-Liss, Inc. and the American Pharmacists Association J Pharm Sci 100:594–603, 2011

Keywords: Piracetam; polymorphism; thermodynamics; thermal analysis; calorimetry; Knudsen effusion; enthalpy of formation

INTRODUCTION

Piracetam (2-oxo-pyrrolidineacetamide, CAS number [7491-74-91]; Fig. 1) is a cyclic derivative of the neurotransmitter γ-aminobutyric acid (GABA) that was synthesized for the first time in 1963.[1] Chemically, piracetam belongs to the pyrrolidone (2-oxopyrrolidine) family and was one of the first compounds classified as a nootropic drug (from the Greek "noos" and "tropein," meaning "mind" and "toward," respectively), a term which refers to an agent that acts on the cognitive function without causing sedation or stimulation.[2] Piracetam also exhibits antithrombotic properties and in fact, a variety of neuronal and vascular effects of piracetam have been reported.[1,2]

For therapeutic uses, the compound is normally marketed as solid dosage forms and, in this case, the possible occurrence of polymorphism becomes a fundamental issue. Indeed, different polymorphs often exhibit significantly different physical properties, such as the fusion temperature, the solubility, or the dissolution rate in a given media.[3–5] These properties may ultimately affect the production and processing of a drug or its bioavailability, if the bioavailability is dissolution limited. The stability hierarchy of the identified polymorphs is also relevant, since they can often coexist under the same temperature and pressure conditions, but there will always be a tendency for all forms to convert over time into the most thermodynamically stable one. This has obvious

Abbreviations used: ΔT_{ad}, adiabatic temperature change; σ, collision diameter; $\Delta_c U_m^\circ$, standard molar energy of combustion; $\Delta_c H_m^\circ$, standard molar enthalpy of combustion; $\Delta_f H_m^\circ$, standard molar enthalpy of formation; $\Delta_{fus} H_m^\circ$, standard molar enthalpy of fusion; $\Delta_{sol} H_m^\circ$, standard molar enthalpy of solution; $\Delta_{sub} H_m^\circ$, standard molar enthalpy of sublimation; $\Delta_{trs} H_m^\circ$, standard molar enthalpy of transition; $\Delta_{trs} S_m^\circ$, standard molar entropy of transition; $\Delta_{trs} G_m^\circ$, standard molar Gibbs energy of transition; $C_{p,m}^\circ$, standard molar heat capacity.

Additional Supporting Information may be found in the online version of this article. Supporting Information

Correspondence to: Hermínio P. Diogo (Telephone: +351-21-8419132; Fax: +351-21-8464457; E-mail: hdiogo@ist.utl.pt); Manuel E. Minas da Piedade (+351-21-7500088; E-mail: memp@fc.ul.pt)

Journal of Pharmaceutical Sciences, Vol. 100, 594–603 (2011)

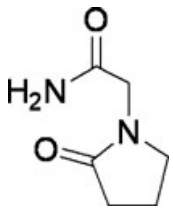

Figure 1. Molecular structure of piracetam.

implications in terms, for example, of the shelf life of a product. The lack of reproducible and tight control of polymorphism can, therefore, render certain formulations unmanufacturable or play havoc with the safe and effective use of an active pharmaceutical ingredient (API).[3–6]

To date, three different polymorphs of piracetam have been isolated at atmospheric pressure (~1 bar), and their molecular and crystal structures published[7]: Form I, monoclinic ($P2_1/n$; $d_{298\,K} = 1.304–1.305$ g·cm^{-3})[8–10]; Form II, triclinic ($P\bar{1}$; $d_{298\,K} = 1.351–1.355$ g·cm^{-3})[8,11]; and Form III, monoclinic ($P2_1/n$; $d_{298\,K} = 1.366–1.386$ g·cm^{-3}).[11–13] Forms II and III can be prepared by crystallization from various solvents (e.g., methanol, propan-2-ol) at ambient temperature.[11,14] When heated to ~400 K, both these phases convert into Form I, which subsequently undergoes fusion at ~435 K.[8,15,16] Form I can be brought to ambient temperature by quenching, but it will revert into Form II within a few hours.[14,16] The rate of this transformation seems, however, to considerably decrease at lower temperatures.[10]

Two additional polymorphs of piracetam, Forms IV and V, that are only stable at high pressures have also been structurally characterized.[10,17] The first one, monoclinic ($P2_1/c$), was obtained by crystallization from aqueous or methanolic solutions at pressures in the range 0.07–0.40 GPa. This polymorph yields Form II on decompression at ambient temperature.[10] Form V, triclinic ($P\bar{1}$), was prepared by direct compression of Form II at ambient temperature and at pressures of 0.7–4.0 GPa.[17]

Besides the five piracetam phases whose molecular and crystal structures were determined, three others, which readily transform into Form II on storage at ambient temperature and pressure, have been postulated based on morphological and optical polarization differences experimentally observed by thermomicroscopy.[8] Some 10 thermodynamically plausible crystalline structures (structures with energies within 5 kJ·mol^{-1} from that corresponding to a global minimum) of piracetam, so far unreported experimentally, have also been predicted by computational methods.[9,18] This suggests that the number of polymorphs of piracetam that may be isolated and structurally characterized is probably not a closed case. Nevertheless, up to now, Forms I–III have been those of most practical relevance.

It is generally accepted that Form I is less stable than Forms II and III at ambient temperature and pressure. However, some controversy exists about the relative thermodynamic stability of polymorphs II and III under those conditions.[8,16,19] Kuhnert-Brandstätter et al.[8] proposed the stability order III > II based, essentially, on the following evidence: (a) on heating Form III from the ambient temperature at a very slow rate, the sequence fusion of Form III (413.2 K) → crystallization of Form II → fusion of Form II (413.7 K) was observed by thermomicroscopy. (b) Despite intensive stirring during 3 days at ~295 K, independent suspensions of Forms II and III in dioxane remained unchanged but, under the same conditions, a 50% (w/w) mixture of both modifications completely converted into Form III. In contrast, the stability hierarchy II > III was deduced by Céolin et al.[16,19] from a semiquantitative pressure–temperature diagram built from topological rules[20] on the assumption that the system is strictly trimorphic. The slopes of the phase boundaries were defined by Clapeyron's equation ($dp/dT = \Delta_{trs}H_m/T\Delta_{trs}V_m$) and calculated by using temperatures and enthalpies ($\Delta_{trs}H_m$) of solid–solid or fusion phase transitions determined by differential scanning calorimetry (DSC), and the corresponding volume changes, $\Delta_{trs}V_m$, obtained from direct density measurements or X-ray diffraction analysis. The obtained conclusions can, however, change if other known high-pressure phases of piracetam are considered.

In this work, the stability hierarchy of Forms I, II, and III of piracetam at 298.15 K was investigated by DSC and solution calorimetry. The obtained results, combined with those of combustion calorimetry, drop-sublimation Calvet microcalorimetry, and Knudsen effusion experiments, allowed the standard molar enthalpies of formation of piracetam in the solid phases I, II, and III and also in the gaseous state to be derived. This last value was finally used to assess the predictions of computational chemistry calculations based on density functional theory (DFT),[21] Gaussian-3 theory with second-order Møller-Plesset (G3MP2),[22] and complete basis set quadratic Becke3 (CBS-QB3)[23,24] methods.

MATERIALS AND METHODS

General

Elemental analyses were carried out with a Fisons Instruments EA1108 apparatus (Fisions Instruments, Madrid, Spain). Fourier transform infrared spectra (FTIR) were recorded in KBr pellets using a Jasco FT/IR 4100 spectrophotometer (Jasco UK, Essex, U.K.) calibrated with polystyrene film. The ^{1}H NMR spectra were obtained in $CDCl_3$ (Aldrich®, 99.9%, containing 0.03% v/v TMS) at ambient temperature, on a

Bruker UltraShield 400 MHz spectrometer (Bruker AXS S.A., France). The X-ray powder diffraction analyses were performed on a Bruker AXS D8 Advance diffractometer (Bruker AXS GmbH, Karlsruhe, Germany) with automatic data acquisition. A Cu Kα radiation source ($\lambda = 1.5418$ Å) was used. The tube amperage was 30 mA and the voltage 40 kV. The diffractograms were recorded in the range $10^\circ \leq 2\theta \leq 50^\circ$, in the continuous mode, with a step size of $0.02^\circ(2\theta)$ and an acquisition time of 2.0 s/step. The sample was mounted on an aluminum sample holder. The indexation of the powder pattern was performed using the program Checkcell.[25]

Materials

A commercial sample of Form III (monoclinic) piracetam (Sigma, 99.5%; CAS number [7491-74-9]) was used without further purification. Elemental analysis for $C_6H_{10}O_2N_2$ (mass fraction): expected C 0.5069, H 0.0709, N 0.1971; found (average of two determinations): C 0.5081, H 0.0714, N 0.1984. ^{1}H NMR (400 MHz, $CDCl_3$/TMS): δ/ppm = 2.07–2.13 (qui, C**H$_2$**, 2H), 2.42–246 (*t*, C**H$_2$**, 2H), 3.45–3.54 (*t*, C**H$_2$**, 2H), 3.94 (*s*, C**H$_2$**, 2H), 5.57 (*s*, N**H$_2$**, 1H), 6.20 (*s*, N**H$_2$**, 1H). These results are compatible with those previously obtained in DMSO.[26] ^{13}C NMR (100 MHz, $CDCl_3$/TMS): δ/ppm = 176.0 (**CO**, ring amide, 1C), 170.4 (**CO**, acetamide, 1C), 48.4 (**C**H$_2$, 1C), 46.8 (**C**H$_2$-ring, 1C), 30.4 (**C**H$_2$-ring, 1C), 18.0 (**C**H$_2$-ring, 1C). FTIR (KBr, main peaks): $\tilde{\nu}$/cm^{-1} = 3342 (ν_{N-H}); 3171 (ν_{N-H}); 2996 (ν_{C-H}, antisymmetric); 2931 (ν_{C-H}); 2880 (ν_{C-H}); 2842 (ν_{C-H}); 2816 (ν_{C-H}); 2760 (ν_{C-H}, symmetric); 1699 ($\nu_{C=O}$, ring); 1658 ($\nu_{C=O}$, acetamide); 1494 (ν_{C-N}); 1470 (ν_{N-C-H}); 1455 (ν_{H-C-C}); 1331 (ν_{C-N-H}); 1290(ν_{C-N}); 902 (ν_{H-N-C}); 862(ν_{C-N}). The powder pattern, obtained at 295 ± 1 K, was indexed as monoclinic, space group $P2_1/n$, with $a = 6.53$ Å, $b = 6.44$ Å, $c = 16.44$ Å, and $\beta = 92.17^\circ$ (see Supporting Information). These results are in good agreement with those previously reported from single crystal X-ray diffraction analysis of Form III piracetam, carried out at ~293 K: $P2_1/n$, $a = 6.49$ Å, $b = 6.41$ Å, $c = 16.38$ Å, and $\beta = 92.21^\circ$[12]; $a = 6.53$ Å, $b = 6.44$ Å, $c = 16.46$ Å, and $\beta = 92.19^\circ$[11]; $a = 6.50$ Å, $b = 6.427$ Å, $c = 16.40$ Å, and $\beta = 92.05^\circ$.[13]

Form II (triclinic) was obtained by two consecutive sublimations of the commercial Form III, at 413 K and 5 Pa. Elemental analysis for $C_6H_{10}O_2N_2$ (mass fraction): C 0.5087, H 0.0726, N 0.1990. FTIR (KBr, main peaks): $\tilde{\nu}$/cm^{-1} = 3346 (ν_{N-H}); 3172 (ν_{N-H}); 3002 (ν_{C-H}, antisymmetric); 2928 (ν_{C-H}); 2874 (ν_{C-H}); 2838 (ν_{C-H}); 2815 (ν_{C-H}); 2763 (ν_{C-H}, symmetric); 1696 ($\nu_{C=O}$, ring); 1661 ($\nu_{C=O}$, acetamide); 1489 (ν_{C-N}); 1466 (ν_{N-C-H}); 1450 (ν_{H-C-C}); 1334 (ν_{C-N-H}); 1293(ν_{C-N}); 898 (ν_{H-N-C}); 865(ν_{C-N}). The powder pattern, obtained at 295 ± 1 K, was indexed as triclinic, space group $P\bar{1}$, with $a = 6.42$ Å, $b = 6.71$ Å, $c = 8.73$ Å, and $\alpha = 80.35^\circ$, $\beta = 103.60^\circ$, $\gamma = 89.25^\circ$ (see Supporting Information). These values are in good agreement with those previously reported from single crystal X-ray diffraction experiments carried out on Form II piracetam at ~293 K: $P\bar{1}$, $a = 6.40$ Å, $b = 6.62$ Å, $c = 8.56$ Å, and $\alpha = 79.85^\circ$, $\beta = 102.39^\circ$, $\gamma = 91.09^\circ$.[11]

The presence of water in the samples of Forms II and III was ruled out by the absence of the characteristic bands at 3408, 1644, and 700 cm^{-1}.[27]

Differential Scanning Calorimetry

The determination of the temperatures and enthalpies of fusion and solid–solid phase transition by DSC was made with a temperature-modulated TA Instruments 2920 MTDSC apparatus (TA Instruments. Guyancourt, France), operated as a conventional DSC. The samples, with masses in the range 2.8–5.6 mg, were sealed under air, in aluminum pans, and weighed to ±0.1 μg on a Mettler UMT2 ultra-micro balance (Mettler-Toledo GmbH, Giessen, Germany). Helium (Air Liquide N55) at a flow rate of 0.5 cm^3·s^{-1} was used as the purging gas. The heating rate was $\beta = 5$ K·min^{-1}. The temperature calibration was performed at the same heating rate by taking the onset of the fusion peaks of the following standards: *n*-decane (Fluka, >99.8%; $T_{fus} = 243.75$ K), *n*-octadecane (Fluka, >99.9%; $T_{fus} = 301.77$ K), hexatriacontane (Fluka, >99.5%; $T_{fus} = 347.30$ K), indium (TA Instruments, DSC standard; $T_{fus} = 430.61$ K), and tin (TA Instruments, DSC standard; $T_{fus} = 506.03$ K). The heat flow scale of the instrument was calibrated by using indium ($\Delta_{fus}h^\circ = 28.71$ J.g^{-1}).[28]

Solution Calorimetry

The standard molar enthalpies of solution of Forms II and III piracetam in distilled and deionized water, at 298.15 K, were measured by using an isoperibol Thermometric Precision Solution Calorimeter (Thermometric AB, Sweden) adapted to a thermal activity monitor thermostat. The apparatus had been previously tested by measuring the enthalpy of solution of tris(hydroxymethyl)aminomethane in NaOH 0.05 mol·dm^{-3} and HCl 0.1 mol·dm^{-3}, and KCl in water.[29,30] The calorimetric cell consisted of a 100 cm^3 Pyrex glass vessel supporting a 30 kΩ thermistor for temperature measurement and a 50 Ω resistance for electrical calibration. The stirrer, which also served as the ampule holder, was operated at 400 rpm. In a typical experiment, a thin-walled 1 cm^3 glass ampule was loaded with ~400 mg of sample and weighed to ±0.01 mg in a Mettler AT201 balance. The solution process was started by breaking the ampule in 100 cm^3 of distilled and deionized water. Electrical calibrations, in which a potential difference of ~5 V was applied to the calibration resistance during ~27 s,

were made before and after the solution process. The energy equivalent of the calorimetric system and the adiabatic temperature change[31] were calculated using the SolCal 1.2 program from Thermometric. The heat associated with ampule breaking was not taken into account because it was found to be negligible in previous experiments where the solvent had a higher vapor pressure than water.[29]

Drop-Sublimation Calvet Microcalorimetry

The enthalpy of sublimation of Form II piracetam was determined by using the electrically calibrated twin-cell drop-sublimation Calvet microcalorimeter (Setaram, Lyon, France) and the operating procedure previously reported.[32,33] The temperature of the calorimeter was set to 365.2 K. In a typical experiment, the sample with a mass in the range 2.0–5.4 mg was placed into a small glass capillary and weighed with a precision of 1 μg in a Mettler M5 microbalance. The capillary was equilibrated for ~10 min, at 298.15 K, inside a furnace placed above the entrance of the sample cell, and subsequently dropped into the cell under N_2 atmosphere. An endothermic peak due to the heating of the compound and capillary from 298.15 to 365.2 K was first observed. Evacuation of the sample and reference cells to 0.13 Pa was started when the signal returned to the baseline and the measuring curve corresponding to the enthalpy of sublimation of the compound at 355.2 K was obtained. The corresponding enthalpy of sublimation (Eq. 1) was derived from the area of that curve, A, the area of the pumping background contribution, A_b, the energy equivalent of the apparatus, $<\varepsilon>$, and the mass of sample m. The value of $<A_b>$ was determined in a series of independent experiments where gaseous nitrogen was pumped out of the cells and $<\varepsilon>$ was obtained by electrical calibration[32]:

$$\Delta_{sub}h = \frac{A_s - < A_b >}{m < \varepsilon >} \quad (1)$$

No decomposition or unsublimed residues were found inside the calorimeter at the end of the experiments. The mean value of the heat capacity of piracetam (Form II) in the range 298.15 to 365.2 K could also be determined, in each experiment, from the area of the first peak observed in the measuring curve, after accounting for the contribution of the glass capillary.[33]

Knudsen Effusion

The Knudsen effusion method was also used to obtain the enthalpy of sublimation of piracetam (Form II) from vapor pressure against temperature measurements. The apparatus and operating procedure were previously described.[34–37] The bottom of the vacuum chamber consisted of a brass block in which up to three effusion cells can be inserted. Only two cells were used in this case. Three temperature sensors were embedded in the block in a triangular configuration: a K-type thermocouple linked to a Eurotherm 902P thermostatic unit and two Tecnisis 100 Ω platinum resistance thermometers connected in a four-wire configuration to a Keithley 2000 multimeter. These sensors were calibrated against a standard platinum resistance thermometer, which had been standardized at an accredited facility in accordance with the International Temperature Scale ITS-90. The temperature of the brass block were maintained constant to better than ±0.1 K by means of a surrounding tubular furnace controlled by the Eurotherm 902P thermostatic unit. The mean value of the block temperature given by the two platinum resistance thermometers was taken as the equilibrium temperature inside the cells. Each cell was initially charged with ~0.2 g of sample, and the mass loss during a run was determined to ±0.01 mg with a Mettler AT201 balance. Before evacuation of the vacuum chamber, the cells were thermally equilibrated with the block for 45–60 min, under nitrogen atmosphere. Typically, a pressure of 1×10^{-3} Pa was reached in less than 3 min, and a final constant pressure of 8×10^{-5} Pa was attained in about 20 min. The experiment was ended by stopping the pumping, and filling the vacuum chamber with nitrogen.

Combustion Calorimetry

The standard energy of combustion of piracetam (Form II) was measured with an isoperibol-stirred liquid combustion macrocalorimeter.[38] A pellet of the compound with a mass of 0.8–0.9 g was weighed to ±0.01 mg with a Mettler AT201 balance inside a platinum crucible, which was then adjusted to the sample holder in the bomb head. The platinum ignition wire (Johnson Matthey; mass fraction: 0.9995; diameter 0.05 mm) was connected between the two discharge electrodes. A cotton thread fuse of empirical formula $CH_{1.887}O_{0.902}$ and standard massic energy of combustion $\Delta_c u^\circ = -16{,}565.9 \pm 8.6$ J·g^{-1},[38] was weighed to ±0.1 μg with a Mettler UMT2 balance. One end of the fuse was tied to the ignition wire and the other end was brought into contact with the pellet. A volume of 1.0 cm^3 of distilled and deionized water from a Millipore system (conductivity, <0.1 μS·cm^{-1}) was added to the bomb body by means of a volumetric pipette. The stainless-steel bomb (Parr 1108) of 340 cm^3 internal volume was assembled and purged twice by successively charging it with oxygen at a pressure of 1.01 MPa and venting the overpressure. After purging, the bomb was charged with oxygen at a pressure of 3.04 MPa and a few minutes were allowed for equilibration before closing the inlet valve. The bomb was placed in the calorimeter proper, inside the

thermostatic bath. The combustion of the sample was initiated by discharge of a 2990 μF capacitor, from a potential of 40 V, through the platinum wire. The discharge current heated the wire, and when the temperature was increased sufficiently, the thread fuse ignited and the combustion propagated to the sample material. The nitric acid formed in the calorimetric experiments from the combustion of the sample or traces of atmospheric N_2 remaining inside the bomb after purging was determined by titration with aqueous sodium hydroxide (Merck titrisol, 0.01 mol·dm^{-3}), using methyl red as an indicator. The energy equivalent of the calorimeter, $\varepsilon^\circ = 18{,}539.88 \pm 0.92$ J·K^{-1}, was obtained from the combustion of benzoic acid (BA; NIST SRM 39j), whose massic energy of combustion under the certificate conditions was $\Delta_c u$(BA, cert) = −26,434 ± 3 J·g^{-1}. The ε° value refers to 3751.38 g of distilled water inside the calorimeter proper.

Computational Details

Density functional theory (DFT),[21] Gaussian-3 theory with second-order Møller-Plesset (G3MP2),[22] and complete basis set extrapolation (CBS-QB3)[23,24] procedures were applied to predict thermochemical properties of the systems under examination. In the case of the DFT methods, full geometry optimizations and frequency predictions were carried out with the B3LYP[39,40] hybrid functional using the cc-pVTZ[41,42] basis set. The corresponding molecular energies were converted to standard enthalpies at 298.15 K by using zero-point energy (ZPE), and thermal energy corrections calculated at the same level of theory. The obtained vibration frequencies and ZPEs were not scaled, unless otherwise stated. The DFT, G3MP2, and CBS-QB3 calculations were performed with the Gaussian-03 package.[43]

RESULTS AND DISCUSSION

The 2005 IUPAC recommended standard atomic masses were used in the calculation of all molar quantities.[44]

Relative Thermodynamic Stability of Piracetam Polymorphs

Typical DSC measuring curves obtained for Forms II and III piracetam at 5 K·min^{-1} are illustrated in Figure 2. The curves show two clear endothermic events, the first one shifted in temperature for Forms II and III and the second one occurring at essentially the same temperature for both forms. This is consistent with previous findings, indicating that Forms II and III first transform into phase I, which subsequently undergoes fusion.[8,16] A very weak endothermic effect can also be noted in the DSC trace of form III (Fig. 2b). This thermal event has been previously observed to sometimes (but not always)

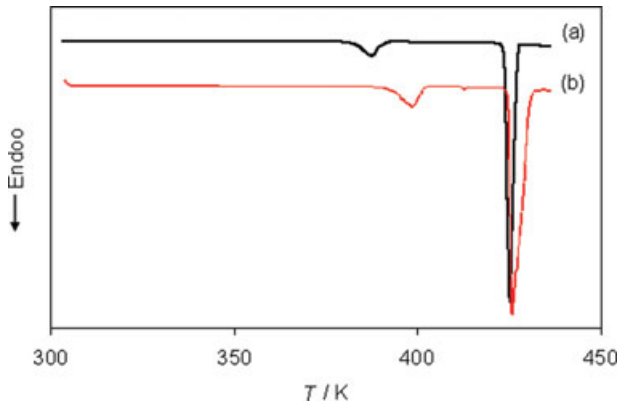

Figure 2. Differential scanning calorimetry measuring curves obtained for forms II (a) and III (b) of piracetam.

occur in DSC studies of form III[16] and may be tentatively assigned to the metastable fusion of traces of form III that remained unconverted after the III → I phase transition. The values of the onset (T_{on}) and maximum (T_{max}) temperatures of the peaks assigned to the II → I or III → I phase transitions and to the fusion of phase I, together with their corresponding enthalpies and entropies ($\Delta_{trs}S^\circ_m = \Delta_{trs}H^\circ_m/T_{trs}$) at the transition temperatures, T_{trs}, are compared in Table 1 with published data resulting from DSC[8,16] and thermomicroscopy[8] experiments. The entropies of the solid–solid phase transitions and fusion obtained in this work were calculated on the assumption that $T_{trs} = T_{on}$. Note that the uncertainties indicated for T_{on}, T_{max}, $\Delta_{trs}H^\circ_m$, and $\Delta_{fus}H^\circ_m$ represent standard deviations of the mean of three independent determinations; those of $\Delta_{trs}S^\circ_m$ and $\Delta_{fus}S^\circ_m$ are overall deviations that include contributions from the uncertainties in the corresponding values of T_{trs} and $\Delta_{trs}H^\circ_m$, or $\Delta_{fus}H^\circ_m$.

As shown in Table 1, the general trends in the temperatures and enthalpies of fusion and solid–solid phase transitions obtained in this work and previously reported are in good agreement. The main exception is the fact that we and Kuhnert-Brandstätter et al.[8] found the order T_{trs}(II → I) < T_{trs}(III → I) whereas the opposite was claimed by Cèolin et al.[16,19] A good agreement is, however, noted when all published enthalpies and entropies for those phase transitions are compared. The stability hierarchy of Forms II and III at 298.15 K can be extracted from the DSC data in Table 1 as follows. Because the final state is identical for the II → I and III → I phase transitions, if the corresponding $\Delta_{trs}H^\circ_m$ and $\Delta_{trs}S^\circ_m$ values obtained at the temperature of the phase transitions are assumed to be temperature independent then $\Delta_{trs}H^\circ_m$ (III → II) = $\Delta_{trs}H^\circ_m$ (III → I) − $\Delta_{trs}H^\circ_m$ (II → I), $\Delta_{trs}S^\circ_m$ (III → II) = $\Delta_{trs}S^\circ_m$ (III → I) − $\Delta_{trs}S^\circ_m$ (II → I), and $\Delta_{trs}G^\circ_m$ (III → II) = $\Delta_{trs}H^\circ_m$ (III → II) − T_{trs}(III → II)$\Delta_{trs}S^\circ_m$ (III → II). The data in Table 1

Table 1. Comparison of the DSC Results Obtained in this Work for Forms II and III Piracetam with Previously Reported Data

Transition	(cr II) → (cr I)	(cr III) → (cr I)	(cr I) → (l)	(cr II) → (l)	(cr III) → (l)
T_{on}/K	382.7 ± 1.2[a]		424.0 ± 0.1[a]		
		394.4 ± 1.2[b]	424.5 ± 0.2[b]		
	381[c]	393[c]	426.4[c]		413.4[c]
	348 ± 2[d]		425.7[d]	413.7[d]	413.2[d]
	399[e]	392[e]	426[e]		412[e]
T_{max}/K	387.9 ± 0.7[a]		425.9 ± 0.4[a]		
		398.9 ± 1.2[b]	425.9 ± 0.2[b]		
ΔH°_{m}/kJ·mol^{-1}	3.23 ± 0.01[a]		25.1 ± 0.1[a]		
		3.73 ± 0.08[b]	26.0 ± 0.1[b]		
	3.0[c]	3.8[c]	25.7 ± 0.3[c]		29.3 ± 0.1[c]
	3.4[e]	4.0[e]	25.6[e]		29.9[e]
ΔS°_{m}/J·K^{-1}·mol^{-1}	8.44 ± 0.04[a]		59.2 ± 0.2[a]		
		9.46 ± 0.20[b]	61.2 ± 0.2[b]		
	7.9 ± 0.8[c]	9.7 ± 0.5[c]	60.3 ± 0.7[c]		70.9 ± 0.2[c]
	8.5[e]	10.2[e]	60.1[e]		72.6[e]

[a] From experiments carried out in this work, where form II was the starting material. [b] From experiments carried out in this work, where form III was the starting material. [c]DSC (differential scanning calorimetry)[8]. [d]Thermomicroscopy[8]. [e]DSC[16].

lead to $\Delta_{trs}H^{\circ}_{m}$ (III → II)/kJ·mol^{-1} = 0.50 (this work), 0.8,[8] and 0.6[16,19]; $\Delta_{trs}S^{\circ}_{m}$ (III → II)/J·K^{-1}·mol^{-1} = 1.02 (this work), 1.8,[8] and 1.7[16,19]; $\Delta_{trs}G^{\circ}_{m}$ (III → II)/kJ·mol^{-1} = 0.20 (this work), 0.3,[8] and 0.1.[16,19] Hence, both the results obtained in this work and published suggest the stability order III > II at 298.15 K.

The value of $\Delta_{trs}H^{\circ}_{m}$ (III → II) at 298.15 K could also be derived from the enthalpies of solution of phases II and III in water obtained by solution calorimetry. These experiments led to $\Delta_{sol}H^{\circ}_{m}$ (cr II) = 13.98 ± 0.09 kJ·mol^{-1} and $\Delta_{sol}H^{\circ}_{m}$ (cr III) = 14.27 ± 0.07 kJ·mol^{-1}, giving $\Delta_{trs}H^{\circ}_{m}$ (III → II) = $\Delta_{sol}H^{\circ}_{m}$ (cr III) − $\Delta_{sol}H^{\circ}_{m}$ (cr II) = 0.29 ± 0.11 kJ·mol^{-1}. This value is close to those obtained by DSC and also corroborates the endothermic nature of the III → II phase transition.

It should be noted that the stability order III > II, at 298.15 K, is further supported by two rules of thumb, which are often used to characterize the relative stability of polymorphs: the density rule and the infrared rule.[4,45] The density rule states that the polymorph with the lower density should be less stable; the infrared rule, when applied to structures containing N−H···O=C hydrogen bonds (such as Forms II and III piracetam),[9,11] indicates that the higher the N−H frequency the weaker the hydrogen bond and the less stable the polymorph. As mentioned in the Introduction, in the case of piracetam $d(\mathrm{III})_{298\,K} > d(\mathrm{II})_{298\,K}$ and the infrared spectroscopy data included in the Materials section shows that $\nu_{N-H}(\mathrm{III}) < \nu_{N-H}(\mathrm{II})$. Thus, both the density and infrared rules suggest that for piracetam Form III is more stable than Form II.

Enthalpies of Sublimation and Formation

The Calvet drop-sublimation microcalorimetry experiments carried out on form II, at 365.2 K, led to $\Delta_{sub}H^{\circ}_{m}$ (365.2 K) = 120.8 ± 1.8 kJ·mol^{-1}, where the indicated uncertainty corresponds to twice the overall standard deviation of the mean of eight independent determinations, including the contributions from the main experiments and from the calibration (see Supporting Information). Correction of this value to 298.15 K gave $\Delta_{sub}H^{\circ}_{m}$ = 123.8 ± 1.8 kJ·mol^{-1}. The correction was based on the equation:

$$\Delta_{sub}H^{\circ}_{m}(298.15\,\mathrm{K}) = \Delta_{sub}H^{\circ}_{m}(T) + \int_{T}^{298.15\,\mathrm{K}} \left[C^{\circ}_{p,m}(g) - C^{\circ}_{p,m}(cr)\right] dT \quad (2)$$

where $C^{\circ}_{p,m}$(cr) and $C^{\circ}_{p,m}$(g) are the standard molar heat capacities of the compound in the crystalline and gaseous states, respectively. The calculation was based on the mean value of the heat capacity of crystalline piracetam in the range 298.15 to 365.2 K, $C^{\circ}_{p,m}(cr) = 206.9 \pm 13.2$ J·K^{-1}·mol^{-1}, determined by Calvet microcalorimetry[33] and on the temperature dependence of the heat capacity of the gaseous compound in the range 200 to 500 K given by:

$$C^{\circ}_{p,m}(g) = 0.4212T + 25.45 \quad (3)$$

Equation 3 was obtained from a least squares fitting to the $C^{\circ}_{p,m}$(g) values calculated by statistical mechanics,[46] using vibration frequencies obtained by the B3LYP/cc-pVTZ method and scaled by 0.965.[47]

The enthalpy of sublimation of piracetam was also obtained from vapor pressure against temperature measurements by the Knudsen effusion method (see Supporting Information). The values of p were calculated from[48,49]:

$$p = \frac{m}{At}\left(\frac{2\pi RT}{M}\right)^{1/2}\left(\frac{8r+3l}{8r}\right)\left(\frac{2\lambda}{2\lambda+0.48r}\right) \quad (4)$$

where m is the mass loss during the time t; A, l, and r are the area, the thickness, and the radius of the effusion hole, respectively; M is the molar mass of the compound under study, R is the gas constant, T is the absolute temperature, and λ is the mean-free path given by[50]:

$$\lambda = \frac{kT}{\sqrt{2}\pi\sigma^2 p} \quad (5)$$

Here k represents the Boltzmann constant and σ the collision diameter. The collision diameter was estimated as 630 pm from the van der Waals volume of each molecule calculated with the GEPOL93 program,[51] based on the molecular structures of the most stable conformations calculated in this work for each compound by the B3LYP/cc-pVTZ method. The van der Waals radii of carbon (170 pm), hydrogen (120 pm), nitrogen (155 pm), and oxygen (152 pm) given by Bondi were selected for this calculation.[52] The area (A), thickness (l), and radii (r) of the two effusion holes used in the measurements were: $A = 2.089 \times 10^{-7}$ m^2, $l = 2.09 \times 10^{-5}$ m; $r = 2.579 \times 10^{-4}$ m (hole 1); $A = 2.640 \times 10^{-7}$ m^2, $l = 2.09 \times 10^{-5}$ m; $r = 2.899 \times 10^{-4}$ m (hole 2).

Since the mean-free path in Eq. 5 is pressure dependent, an iterative method was needed to obtain the vapor pressure of the compound through Eqs. 4 and 5. As a first approximation, p was calculated by ignoring the λ-dependent term in Eq. 4. The obtained result was subsequently used to derive λ from Eq. 5. The calculated mean-free path was introduced in Eq. 4 and a second p value was calculated. The iteration was continued until the difference between successive values of p was smaller than 10^{-8} Pa.

The vapor pressure against temperature data was fitted to Eq. 6, [53]:

$$\ln p = a - \frac{b}{T} \quad (6)$$

where the slope b is related to the enthalpy of sublimation at the average of the highest and lowest temperatures of the range covered in each series of experiments, T_m, by $\Delta_{sub}H^\circ_m(T_m) = bR$. The obtained results were: $a = 36.99 \pm 0.76$, $b = 14{,}235.3 \pm 278.2$, $\Delta_{sub}H^\circ_m$ (365.4 K) $= 118.4 \pm 5.0$ kJ·mol^{-1} (hole 1); $a = 36.58 \pm 0.39$, $b = 14{,}098.7 \pm 142.6$, $\Delta_{sub}H^\circ_m$ (365.4 K) $= 117.2 \pm 2.6$ kJ·mol^{-1} (hole 2). The uncertainties assigned to a and b correspond to standard errors, and that of $\Delta_{sub}H^\circ_m(T_m)$ includes Student's factor for 95% confidence level (hole 1: $t = 2.179$ for 13 experimental points; hole 2: $t = 2.228$ for 11 experimental points).[54] Correction of the obtained $\Delta_{sub}H^\circ_m$ (365.4 K) values to 298.15 K using Eq. 2 led to $\Delta_{sub}H^\circ_m$ (cr II) $= 121.4 \pm 5.0$ kJ·mol^{-1} (hole 1) and $\Delta_{sub}H^\circ_m$ (cr II) $= 120.2 \pm 2.6$ kJ·mol^{-1} (hole 2). The weighted mean[55] of the results from the Calvet drop-sublimation microcalorimetry and the Knudsen effusion experiments $\Delta_{sub}H^\circ_m$ (cr II) $= 122.5 \pm 1.4$ kJ·mol^{-1} was selected in this work.

Eight combustion calorimetry experiments on Form II piracetam (see Supporting Information) led to a mean value of the standard-specific energy combustion $\Delta_c u^\circ$ (cr II) $= -22{,}969.16 \pm 3.64$ J·g^{-1}, from which $\Delta_c U^\circ_m$ (cr II) $= -3265.20 \pm 1.32$ kJ·mol^{-1} and $\Delta_c H^\circ_m$ (cr II) $= -3266.44 \pm 1.32$ kJ·mol^{-1} can be derived. According to normal thermochemical practice, the uncertainties assigned to $\Delta_c u^\circ$ (cr II) are the standard deviations of the mean and those of $\Delta_c U^\circ_m$ (cr II) and $\Delta_c H^\circ_m$ (cr II) represent twice the overall standard deviation of the mean including the contributions from the main experiments and from the calibration with benzoic acid[55,56].

The value of $\Delta_c H^\circ_m$ (cr II) corresponds to the reaction:

$$C_6H_{10}O_2N_2\,(cr) + 15/2O_2\,(g) = 6CO_2\,(g) + 5H_2O\,(l) + N_2\,(g) \quad (7)$$

and using $\Delta_f H^\circ_m$ (CO_2, g) $= -393.51 \pm 0.13$ kJ·mol^{-1},[57] and $\Delta_f H^\circ_m$ (H_2O, l) $= -285.830 \pm 0.040$ kJ·mol^{-1}[57] leads to $\Delta_f H^\circ_m$ (cr II) $= -523.8 \pm 1.6$ kJ·mol^{-1}. Combining this value with the enthalpies of solution of Forms II and III piracetam indicated above leads to $\Delta_f H^\circ_m$ (cr III) $= \Delta_f H^\circ_m$ (cr II) $+ \Delta_{sol}H^\circ_m$ (cr II) $- \Delta_{sol}H^\circ_m$ (cr III) $= -524.1 \pm 1.6$ kJ·mol^{-1}. A similar exercise based on the assumption that the enthalpy of the II → I phase transition obtained by DSC, $\Delta_{trs}H^\circ_m$ (II → I) $= 3.21 \pm 0.04$ kJ·mol^{-1} (Table 1), is invariant with temperature gives $\Delta_f H^\circ_m$ (cr I) $= \Delta_f H^\circ_m$ (cr II) $+ \Delta_{trs}H^\circ_m$ (II → I) $= -520.6 \pm 1.6$ kJ·mol^{-1}. Finally, the standard molar enthalpy of formation of gaseous piracetam could be derived as $\Delta_f H^\circ_m$ (g) $= -401.3 \pm 2.1$ kJ·mol^{-1} by using $\Delta_f H^\circ_m$ (cr II) and $\Delta_{sub}H^\circ_m$ (cr II) $= 122.5 \pm 1.4$ kJ·mol^{-1} proposed in this work.

Computational Chemistry

The experimentally obtained $\Delta_f H^\circ_m$ (g) value can be compared with the corresponding predictions by the B3LYP/cc-pVTZ, $\Delta_f H^\circ_m$ (g) $= -335.3$ kJ·mol^{-1}, G3MP2, $\Delta_f H^\circ_m$ (g) $= -388.7$ kJ·mol^{-1}, and CBS-QB3, $\Delta_f H^\circ_m$ (g) $= -402.8$ kJ·mol^{-1} methods for the most stable conformation of gaseous piracetam (Fig. 3). This conformation involves a NH···O intramolecular hydrogen bond, with the calculated H···O bond distance being 210.3 pm, 213.8 pm, and 209.9 pm, at the B3LYP/cc-pVTZ, G3MP2, and CBS-QB3 levels of theory, respectively. The theoretical $\Delta_f H^\circ_m$ (g) results were based on the enthalpy of the atomization reaction, $\Delta_a H^\circ_m$:

$$C_6H_{10}O_2N_2(g) = 6C(g) + 10H(g) + 2O(g) + 2N(g) \quad (8)$$

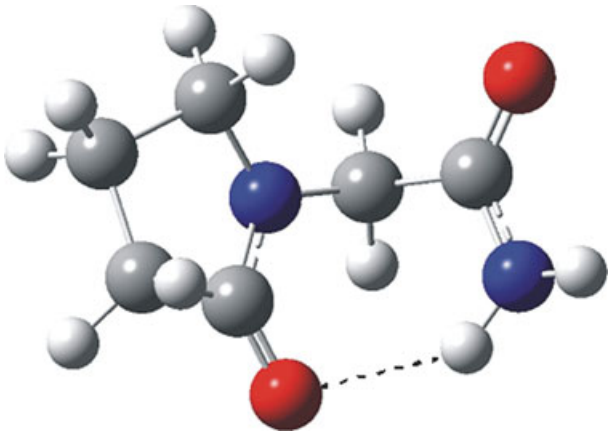

Figure 3. Most stable conformation of gaseous piracetam displaying the intramolecular NH···O hydrogen bond.

computed at 298.15 K as $\Delta_a H^\circ_m = 8259.0$ kJ·mol^{-1}, $\Delta_a H^\circ_m = 8312.4$ kJ·mol^{-1}, and $\Delta_a H^\circ_m = 8326.5$ kJ·mol^{-1} at the B3LYP/cc-pVTZ, G3MP2, and CBS-QB3 levels of theory, respectively (see Supporting Information for details).

The deviations found between the experimental and calculated $\Delta_f H^\circ_m$ (g) values amount to 66.1 kJ·mol^{-1} (B3LYP/cc-pVTZ), 12.7 kJ·mol^{-1} (G3MP2), and 1.4 kJ·mol^{-1} (CBS-QB3). The poor performance of the DFT model is not unexpected.[21,58–60] In fact, a recent assessment showed that on average deviations of at least ~30 kJ·mol^{-1} should be expected when predicting $\Delta_f H^\circ_m$ (g) from atomization enthalpies at the B3LYP/cc-pVTZ level of theory.[60] Considerable improvements are, however, observed when the higher level G3MP2 and particularly CBS-QB3 methods are used. This last method was able to reproduce the experimental data within its uncertainty interval.

CONCLUSIONS

Besides the assessment of computational chemistry methods that are frequently used to investigate the energetics, structure, and reactivity of molecules with pharmaceutical interest, the combination of experimental techniques used in this work provided some basic thermodynamic information (e.g., enthalpies of formation, vapor pressures) that was lacking for the three piracetam polymorphs that have been of most practical relevance (Forms I, II, and III). Last but not the least, the stability hierarchy of those forms at ambient temperature and pressure (298 K, 1 bar), for which there was conflicting evidence in the literature, could be deduced as III > II > I. This conclusion is in line with the predictions of the density and infrared rules.

Supporting Information: Tables S1 and S2 containing the details of the X-ray powder diffraction characterization of Forms II and III of piracetam. Tables S3 and S4 summarizing the results of the solution calorimetry measurements. Table S5 with the results of the drop-sublimation Calvet microcalorimetry experiments. Table S6 containing the experimental vapor pressures obtained by the Knudsen effusion method. Details of the combustion calorimetry experiments (Table S7). Details of the computational chemistry calculations (Table S8). Supporting information is available free of charge via the Internet (http://wileyonlinelibrary.com/).

ACKNOWLEDGMENTS

This work was supported by Fundação para a Ciência e a Tecnologia, Portugal (Project PTDC/QUI-QUI/098216/2008). A PhD grant from FCT is gratefully acknowledged by R. Picciochi (SFRH/BD/36029/2007). Thanks are also due to Profs. J. J. Moura Ramos (IST, Portugal) and F. Martins (FCUL, Portugal) for the use of the DSC apparatus and the solution calorimeter, respectively, and to Dr. C. E. S. Bernardes (IST, Portugal) for the NMR analysis.

REFERENCES

1. Gouliaev AH, Senning A. 1994. Piracetam and other structurally related nootropics. Brain Res Rev 19(2):180–222.
2. Winblad B. 2005. Piracetam: A review of pharmacological properties and clinical uses. CNS Drug Rev 11(2):169–182.
3. Brittain HG. Ed. 1999. Polymorphism in pharmaceutical solids. New York: Marcel Dekker.
4. Bernstein J. 2002. Polymorphism in molecular crystals. Oxford: Oxford University Press.
5. Hilfiker R. 2006. Polymorphism in the pharmaceutical industry. Weinheim: Wiley-VCH.
6. Bauer J, Spanton S, Henry R, Quick J, Dziki W, Porter W, Morris J. 2001. Ritonavir: An extraordinary example of conformational polymorphism. Pharm Res 18(6):859–866.
7. Allen FH. 2002. Cambridge structural database. Acta Crystallogr B58:380–388.
8. Kuhnert-Brandstätter M, Burger A, Völlenklee R. 1994. Stability behaviour of piracetam polymorphs. Sci Pharm 62:307–316.
9. Louër D, Louër M, Dzyabchenko VA, Agafonov V, Céolin R. 1995. Structure of a metastable phase of piracetam from X-ray-powder diffraction using atom-atom potential method. Acta Crystallogr B51:182–187.
10. Fabbiani FPA, Allan DR, Parsons S, Pulham CR. 2005. An exploration of the polymorphism of piracetam using high pressure. Cryst Eng Comm 7:179–186.
11. Admiraal G, Eikelenboom JC, Vos A. 1982. Structures of the triclinic and monoclinic modifications of (2-oxo-1-pyrrolidinyl)acetamide. Acta Crystallogr B 38:2600–2605.
12. Bandoli G, Clemente DA, Grassi A, Pappalardo GC. 1981. Molecular determinants for drug-receptor interactions.1. Solid-state structure and conformation of the novel nootropic agent 2-pyrrolidone-*N*-acetamide—X-ray and theoretical SCF-MO studies. Mol Pharmacol 20(3):558–564.

13. Gałdecki Z, Główka ML. 1983. Crystal structure of nootropic agent, piracetam—2-oxopyrrolidin-1-ylacetamide. Pol J Chem 57:1307–1312.
14. Pavlova A, Konstantinova K, Daskalov H, Georgiev A. 1983. A study of crystalline forms of piracetam. Pharmazie 38(9):634–634.
15. Pavlova AV. 1984. Kinetics of polymorphic transformation of piracetam crystal forms. Pharmazie 39(4):272–273.
16. Céolin R, Agafonov V, Louer D, Dzyabchenko VA, Toscani S, Cense JM. 1996. Phenomenology of polymorphism, III: p,T diagram and stability of piracetam polymorphs. J Solid State Chem 122(1):186–194.
17. Fabbiani FPA, Allan DR, David WIF, Davidson AJ, Lennie AR, Parsons S, Pulham CR, Warren JE. 2007. High-pressure studies of pharmaceuticals: An exploration of the behavior of piracetam. Cryst Growth Des 7(6):1115–1124.
18. Nowell H, Price SL. 2005. Validation of a search technique for crystal structure prediction of flexible molecules by application to piracetam. Acta Crystallogr B61:558–568.
19. Toscani S. 1998. An up-to-date approach to drug polymorphism. Thermochim Acta 321:73–79.
20. Ceolin R, Toscani S, Agafonov V, Dugue J. 1992. Phenomenology of polymorphism.1. Pressure temperature representation of trimorphism—general rules—application to the case of dimethyl 3,6-dichloro-2,5-dihydroxyterephthalate. J Solid State Chem 98(2):366–378.
21. Koch W, Holthausen MCA. 2002. Chemist's guide to density functional theory. 2nd ed. Weinheim: Wiley-VCH.
22. Curtiss LA, Redfern PC, Raghavachari K, Rassolov V, Pople JA. 1999. Gaussian-3 theory using reduced Moller-Plesset order. J Chem Phys 110(10):4703–4709.
23. Montgomery Jr. JA, Frisch MJ, Ochterski JW, Petersson GA. 1999. A complete basis set model chemistry. VI. Use of density functional geometries and frequencies. J Chem Phys 110:2822–2827.
24. Montgomery Jr. JA, Frisch MJ, Ochterski JW, Petersson GA. 2000. A complete basis set model chemistry. VII. Use of the minimum population localization method. J Chem Phys 112:6532–6542.
25. Laugier J, Bochu B. Chekcell. http://www.ccp14.ac.uk/tutorial/lmgp/chekcell.htm (last accessed: April 23, 2010).
26. Valenta V, Holubek J, Svatek E, Valchar M, Krejci I, Protiva M. 1990. Potential nootropic agents—synthesis of some (2-oxo-1-pyrrolidinyl)acetamides and some related compounds. Collect Czech Chem Commun 55(11):2756–2764.
27. Maréchal Y. 2007. The hydrogen bond and the water molecule: The physics and chemistry of water, aqueous and bio-media. Amsterdam: Elsevier.
28. Moura Ramos JJ, Taveira-Marques R, Diogo HP. 2004. Estimation of the fragility index of indomethacin by DSC using the heating and cooling rate dependency of the glass transition. J Pharm Sci 93(16):1503–1507.
29. Nunes N, Martins F, Leitão RE. 2006. Thermochemistry of 1-bromoadamantane in binary mixtures of water–aprotic solvent. Thermochim Acta 441:27–29.
30. Marsh KN. Ed. 1987. Recommended reference materials for the realization of physicochemical properties. Oxford: IUPAC-Blackwell Scientific Publications.
31. Martinho Simões JA, Minas da Piedade ME. 2008. Molecular energetics. New York: Oxford University Press.
32. Kiyobayashi T, Minas da Piedade ME. 2001. The standard molar enthalpy of sublimation of η^5-bis-pentamethylcyclopentadienyl iron measured with an electrically calibrated vacuum-drop sublimation microcalorimetric apparatus. J Chem Thermodyn 33:11–21.
33. Bernardes CES, Santos LMNBF, Minas da Piedade ME. 2006. A new calorimetric system to measure heat capacities of solids by the drop method. Meas Sci Technol 17:1405–1408.
34. Calado JCG, Dias AR, Minas da Piedade ME, Martinho Simões JA. 1980. Standard enthalpy of sublimation of $[Mo(\eta\text{-}C_5H_5)_2(CH_3)_2]$. A re-evaluation of Mo-$CH_3$ and W-CH_3 bond enthalpy contributions. Rev Port Quim 22: 53–62.
35. Diogo HP, Minas da Piedade ME, Fernandes AC, Martinho Simões JA, Ribeiro da Silva MAV, Monte MJS. 1993. The enthalpy of sublimation of diphenylacetylene from Knudsen effusion studies. Thermochim Acta 228:15–22.
36. Diogo HP, Minas da Piedade ME, Goncalves JM, Monte MJS, Ribeiro da Silva MAV. 2001. Enthalpies of sublimation of $M(\eta^5\text{-}C_5H_5)_2Cl_2$ (M = Ti, Zr, Hf, V, Nb, W) complexes. Eur J Inorg Chem (1):257–262.
37. Gonçalves EM, Bernardes CES, Diogo HP, Minas da Piedade ME. 2010. Energetics and structure of nicotinic acid (Niacin). J Phys Chem B 114:5475–5485.
38. Pinto SS, Diogo HP, Minas da Piedade ME. 2003. Enthalpy of formation of monoclinic 2-hydroxybenzoic acid. J Chem Thermodyn 35:177–188.
39. Becke AD. 1993. Density-functional thermochemistry. 3. The role of exact exchange. J Chem Phys 98:5648–5652.
40. Lee C, Yang W, Parr RG. 1988. Development of the Colle–Salvetti correlation-energy formula into a functional of the electron-density. Phys Rev B 37:785–789.
41. Dunning TH. 1989. Gaussian-basis sets for use in correlated molecular calculations. 1. The atoms boron through neon and hydrogen. J Chem Phys 90(2):1007–1023.
42. Dunning TH, Peterson KA, Wilson AK. 2001. Gaussian basis sets for use in correlated molecular calculations. X. The atoms aluminum through argon revisited. J Chem Phys 114(21):9244–9253.
43. Frisch MJ, Trucks GW, Schlegel HB, Scuseria GE, Robb MA, Cheeseman JR, Montgomery Jr. JA, Vreven T, Kudin KN, Burant JC, Millam JM, Iyengar SS, Tomasi J, Barone V, Mennucci B, Cossi M, Scalmani G, Rega N, Petersson GA, Nakatsuji H, Hada M, Ehara M, Toyota K, Fukuda R, Hasegawa J, Ishida M, Nakajima T, Honda Y, Kitao O, Nakai H, Klene M, Li X, Knox JE, Hratchian HP, Cross JB, Adamo C, Jaramillo J, Gomperts R, Stratmann RE, Yazyev O, Austin AJ, Cammi R, Pomelli C, Ochterski JW, Ayala PY, Morokuma K, Voth GA, Salvador P, Dannenberg JJ, Zakrzewski VG, Dapprich S, Daniels AD, Strain MC, Farkas O, Malick DK, Rabuck AD, Raghavachari K, Foresman JB, Ortiz JV, Cui Q, Baboul AG, Clifford S, Cioslowski J, Stefanov BB, Liu G, Liashenko A, Piskorz P, Komaromi I, Martin RL, Fox DJ, Keith T, Al-Laham MA, Peng CY, Nanayakkara A, Challacombe M, Gill PMW, Johnson B, Chen W, Wong MW, Gonzalez C, Pople JA. 2004. Gaussian 03, Revision C.02. Wallingford: Gaussian, Inc.
44. Wieser ME. 2006. Atomic weights of the elements 2005—(IUPAC technical report). Pure Appl Chem 78(11):2051–2066.
45. Burger A, Ramberger R. 1979. Polymorphism of pharmaceuticals and other molecular crystals. I. Theory of thermodynamic rules. Mikrochim Acta 2(3–4):259–271.
46. Irikura KK, Frurip DJ. 1998. Computational thermochemistry: Prediction and estimation of molecular thermodynamics.Washington: ACS Symposium Series No. 677.
47. Johnson III RD. Ed. 2010. Computational chemistry comparison and benchmark database. NIST standard reference database 101 Gaithersburg: National Institute of Standards and Technology.
48. Edwards JW, Kington GL. 1962. Thermodynamic properties of ferrocene.2. Vapour pressure and latent heat of sublimation at 25°C by effusion and thermistor manometer methods. Trans Farad Soc 58:1323–1333.
49. Andrews JTS, Westrum Jr. EF, Bjerrum N. 1969. Heat capacity and vapor pressure of crystalline bis(benzene)chromium.

Third-law entropy comparison and thermodynamic evidence concerning structure of bis(benzene)chromium. J Organomet Chem 17:293–302.
50. Atkins PW, de Paula J. 2002. Physical chemistry. 7th ed., Oxford: Oxford University Press. pp 822.
51. Pascual-Ahuir JL, Silla E, Tunon I. GEPOL93. Available at: http://www.ccl.net/cca/software/SOURCES/FORTRAN/molecular_surface/gepol93./
52. Bondi A. 1964. Van der Waals Volumes and Radii. J Phys Chem 68(3):441–451.
53. Denbigh K. 1981. The principles of chemical equilibrium. 4th ed., Cambridge: Cambridge University Press.
54. Korn GA, Korn TM. 1968. Mathematical handbook for scientists and engineers. New York: McGraw-Hill.
55. Olofsson G. 1979. Assignment of uncertainties. In Experimental chemical thermodynamics; Sunner S, Månsson M, Eds. London: Pergamon Press. pp 137–159.
56. Bjellerup L. 1961. On the accuracy of heat of combustion data obtained with a precision moving-bomb calorimetric method for organic bromine compounds. Acta Chem Scand 15(15):121–140.
57. Cox JD, Wagman DD, Medvedev VA. 1989. CODATA key values for thermodynamics.New York: Hemisphere Publishing Corp.
58. Boese AD, Martin JML, Handy NC. 2003. The role of the basis set: Assessing density functional theory. J Chem Phys 119(6):3005–3014.
59. Sousa SF, Fernandes PA, Ramos MJ. 2007. General performance of density functionals. J Phys Chem A 111(42):10439–10452.
60. Riley KE, Op't Holt BT, Merz KM. 2007. Critical assessment of the performance of density functional methods for several atomic and molecular properties. J Chem Theory Comput 3(2):407–433.